



Bridging the Implementation Gap in the CZM Protocol: A Method for Coastal Setbacks Determination on Rough Impermeable Shores

A Case Study in Kavala Municipality (N. Greece)

Georgios SYLAIOS, KALLIA-ANTONIOU Aggeliki & ZOIDOU Maria

Department of Environmental Engineering, Democritus University of Thrace, 67100 Xanthi, Greece



Xanthi, 2013

1. Introduction

A coastal setback is a buffer zone defined by a specific distance from the shoreline's highest winter water mark, within which permanent constructions are not allowed. Setback zones consist a coastal zone management tool for a number of different reasons, such as to ensure public access, to protect the ecological and landscape integrity of the coast, but also to minimize the natural risk hazards protecting population and developments (Rochette and Billé, 2010). According to FAO (2006), the determination methods for setback zones definition and the imposed setback rules vary substantially worldwide, in terms of the setback baseline definition, the width of the exclusion zone, the types of the activities and uses excluded or restricted, and the contents and context of the exclusion regime. Different countries have adopted variable setback zone determination methods and widths, varying from 100 m to 1,000 m. In the U.S., coastal setbacks serve as 'no build areas', with significant variability from state to state in their definition (e.g., fixed, erosion-based, or mixed), laws and regulations (Rabenold, 2013).

Setback lines and zones provide opportunities for planners and stakeholders to consider the natural landscape elements along the shore (Cambers, 1997). They were firstly introduced in international treaties by Article 8-2a of the Mediterranean ICZM Protocol aiming to ensure biodiversity protection, to maintain the ecosystem services of coastlines, to preserve cultural and natural assets and traditional landscapes and to protect population and infrastructure from climate change risks (Sanò et al., 2010). Such provision was dictated by the gradually increased human pressures exerted on the Mediterranean coastal zone, since coastal population rises with an annual growth rate of 1.4%, projected at 174 million inhabitants by 2025 (Plan Bleu, 2005); seasonal tourism flows escalate to the projected 350 million tourists (UNEP, 2012); artificial land cover expands at an alarming pace, leading to the concretion of almost 40% of the Mediterranean coasts by urban sprawl, roads, tourist facilities and ports (Pan Bleu, 2005); coastal landscapes and sites of environmental and cultural importance are under constant degradation (Alpan, 2011).

Indeed, the ICZM Protocol identifies in Article 8 that Parties "shall establish in coastal zones, as from the highest winter waterline, a zone where construction is not allowed. Taking into account, *inter alia*, the areas directly and negatively affected by climate change and natural risks, this zone may not be less than 100 meters in width..." (UNEP, 2008). However, a preliminary analysis of the Protocol brings out that no specific unified and integrated guidelines exist for the determination of coastal setback lines and zones, as a mean for their implementation. Furthermore, the fact that most coastlines face or are threatened by coastal erosion and the effects of climate change increases the need for a European Methodological Framework on Coastal Setbacks Definition.

In this report we attempt to propose a scientifically sound methodology, utilizing modern tools and techniques to determine the coastal setback zones and baselines

over the rocky Mediterranean shorelines. The applicability of this methodology is tested along a steep and rocky coastal stretch in Kavala Municipality (Northern Greece). The development and adoption of a common method for setback lines definition appears as a prerequisite of the ICZM Protocol, but it also serves the European cohesion policy, especially for the EU Member States that are contracting parties to the Mediterranean ICZM Protocol (Spain, France, Italy, Slovenia, Greece, Malta, Cyprus). Bridge and Salman (2010) explained that a common problem occurs in delimiting and mapping the setback lines, especially when there is no precise definition of the coastal zone. The baseline, from which to measure the landward or seaward boundary appears variable and often depends on legal definitions of waterlines, coastline/shoreline, and the level of low and high water tides.

Sanó et al. (2010) explained that coastal setbacks and baselines identification should consider the nature and morphology of the coast, and classified Mediterranean coastal stretches into four types, as open sandy coastlines, semi-enclosed coastal lagoons, rocky coastlines and hard infrastructures. Sanó et al. (2011) described the theoretical framework for the technical definition of the high water mark line, especially for sandy beaches, where the impact of coastal erosion and the subsequent coastline retreat and shoreline morphological changes appear significant. Climate impact trends and projections, the influence of the tide and the exposure of the coast to extreme storm surges and waves are the factors to be considered in such analysis. The deliverables of EU funded program named “CONSCIENCE: Concepts and science for Coastal Erosion Management” discussed the use of setback lines for coastal protection in Europe and the Mediterranean and attempted to prepare a set of integrated guidelines for the definition of set-back lines (Conscience, 2010).

2. Coastal Setbacks in Greece

Although the Protocol was adopted in 2008 and entered into force on 24 of March 2011, some Mediterranean countries, like Greece, had already included in their legislation the concept of coastal setback zones. Indeed, the newly established Greek state (1829) adopted by Law 21-6-1837 the public use of coastal zones as a succession from the Byzantine Code of Law and the even earlier Roman Legal Code, from where the term “highest winter waterline” originates (Roman Institute of Justinian of 533, Book II, title I). The objectives and means of the public use of coastal zones were specified later, in article 7 of Law 2344/1940, the main legal framework related to coastal protection and development for most of contemporary history of Greece. In this document a setback zone of 20 m wide was defined, using as baseline the mean sea level datum. L. 2344/1940 was enacted for almost 61 years, putting emphasis on the citizens’ right to enjoy the coastal zone as a public property, than on the obligation of the State to protect the coastal areas as parts of the natural environment and as vulnerable ecosystems. In addition, there were no references on the types of the activities and uses excluded or restricted, on land use controls, protection from urban

sprawl, and the general planning regulations for the coastal zones. Finally, it failed to specify the procedures and the technical means to define the coastal setback lines and zones with acceptable accuracy, leading to long disputes between stakeholders and significant delays in coastal developments.

Through newer legislation, construction was restricted beyond a 30 m distance from the coastline, in urban coastal areas and in old settlements pre-existing 1923 (L.D 439/1970); the legal procedures for demolition of illegal constructions were defined (L.D 393/1974); special plans and programs for the protection of the coastal zone and the sustainable use of natural and cultural environment were introduced (L.360/1976); Development Control Zones with land use restrictions around urban areas and areas of high environmental and archaeological value were designated (L. 1337/1983). Finally, L. 2971/2001 abolished previous provisions and focused on the rational development of coastal areas, protecting the environmental, cultural, social and economic aspects of the coastal zones. This law expanded the coastal setback zone up to 50 m width, using as baseline the maximum potential wave run-up on the sloping beach, as the highest winter water mark. In this zone public access is unlimited, environmental and social goals for public interest should be promoted and all types of construction are prohibited.

However, L. 2971/2001 fails to provide an objective method for the accurate determination of the highest winter water mark, leaving this duty to a committee of administrators derived from the regional public land management service, the regional environmental management department and the local port authority. The Law establishes a set of criteria to be considered for this process, as coastal geomorphology, vegetation seaward limit, local and broader meteorological conditions, maximum wave run-up, sea bottom morphology, wave fetch, existing and planned technical works along the coastline, sensitive ecosystems and vulnerable areas. Although the above criteria involve the use of scientific tools and data, as topographic and bathymetric maps, remote sensing images, meteorological datasets, wave dynamics and fetch lengths, etc., there is a lack of a well-prescribed and scientifically substantiated procedure that will objectively define the maximum potential wave run-up on the coast, and thus accurately determine the highest winter water marks and the subsequent coastal setback zone. The results of this deficiency is a series of legal disputes between coastal property owners, other involved stakeholders, potential coastal developers and the Greek state, leading to improper law enforcement and significant delays in the implementation of coastal development projects.

3. Methodological Framework for Coastal Setbacks Determination

The determination of coastal setbacks is a step-wise procedure in which physical, ecological, socio-economic, administrative and public participation processes should

be considered. Sanó et al. (2010) presented the basis for such methodology, implemented within the framework of the ICZM Protocol, as shown in Figure 1. According to this methodological framework the following stages should be considered for coastal setbacks determination:

Step 1: Geomorphologic Coastal Classification

According to Sanó et al. (2010), each Mediterranean coastal stretch may be classified into one of the four following types: a) open-sea sandy coastlines, in which sandy beaches and coastal dunes prevail. In this type a wide range of beaches may be classified, from the small, pocket beaches to the long sandy beach systems. Waves, storms and climate change impacts affect the long-shore and cross-shore sediment transport of these systems, governing their morphodynamics.

b) semi-enclosed coastal lagoons, covered with finer sediments as fine sands and/or mud. These coasts are more protected from the wave action but hydrodynamic circulation and extreme storm surges are significant in shaping their morphodynamics.

c) rocky coastlines as cliffs and lower bluffs, which in contrast to the previous two types appear stable to coastal erosion, and

d) hard infrastructures, implying any human-made construction is placed on the coastline or substitutes it, as ports, dikes, groins, revetments, airports or artificial islands.

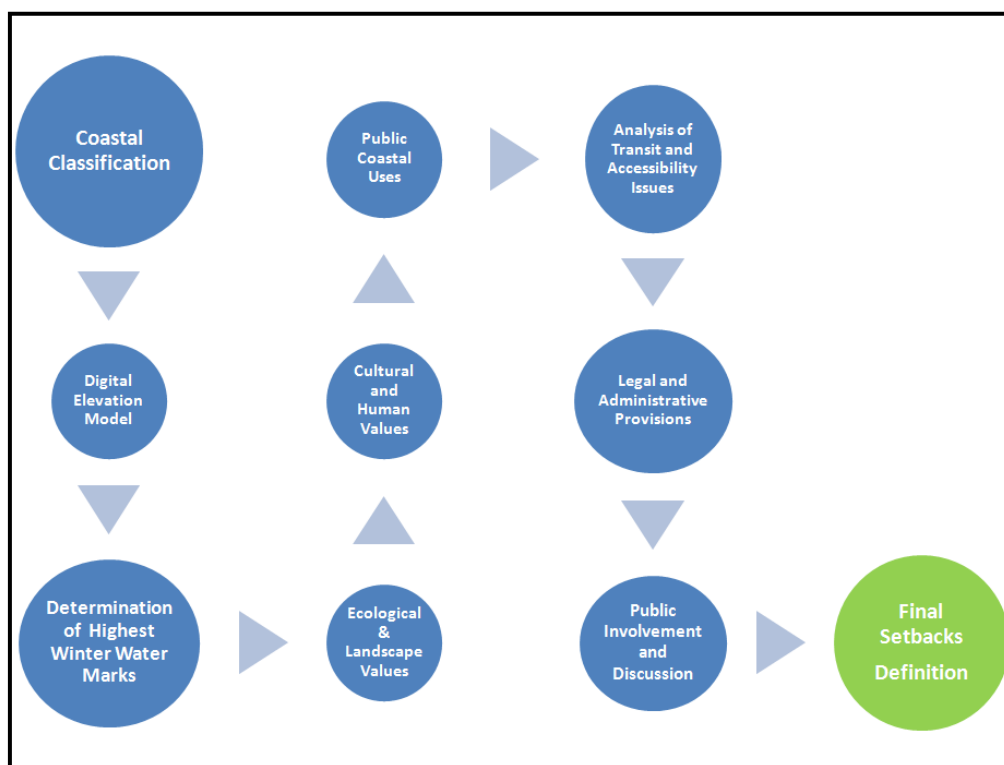


Figure 1. The step-wise process of coastal setbacks definition (after Sanó et al., 2010).

Step 2: Shoreline Digital Elevation Model

Blended bathymetric and topographic data derived from various sources may be utilized and imported in a GIS to comprise an analytical DEM for the examined shoreline. Presently, several instruments and methods for conducting topo-bathymetric surveys exist; however, their accuracy should be extensively evaluated. For the emerged part of the beach, methods as the direct topographic surveying, GPS surveying using geodetic receivers, aerial phtogrammetric survey combined to stereoscopic image analysis, the use of laserscan and finally, the airborne LIDAR scanning are some of the available techniques to produce highly accurate DEMs. These methods were evaluated in terms of their accuracy and survey costs by BeachMed-e program, as shown in the following table.

Table 1. Evaluation of the emerged beach survey methods for DEM development.

Method	Precision	Survey Density	Survey times (km/days)	Survey Cost (€/km)	Notes
Topographic Survey	5 cm	Transects every 50 m	5	800	
Geodetic GPS Survey	5 cm	Transects every 50 m	10	800	
Laser Scanner	5 cm	1 × 1 dm	1	1,500	Only for small beaches
Airborne LIDAR	10 cm	1 × 1 m	50	1,000	Only for long beaches
Aerial Photogrammetry	10 cm	Transects every 1 m	30	600	

For the submerged part of the beach, hydrographic survey echo-sounders (single or multi-beams) with an accuracy of up to 1 cm could be used.

Step 3: Determination of the Highest Winter Water Marks

The methodological framework for the highest winter water marks (HWWMs) and the subsequent coastal setback zone determination is graphically summarized in Figure 2. It is presently known that the highest winter water mark on a coast is determined by the following combined factors: a) the run-up of waves breaking on the coast, with a certain return period, b) the tidal water level during tidal flood, c) the storm surge effect, and d) the morphology of the shoreline, and it's gradual retreat due to the high energy waves, known as beach erosion effect (Sanò et al., 2010). In the case of rocky impermeable shores, this latter impact may be neglected. Thus, the water level fluctuates as:

$$X(t) = Z_0(t) + T(t) + W(t) + S(t) \quad (1)$$

where $Z_0(t)$ is the mean sea level, exhibiting a slow but gradual rise due to climate change, $T(t)$ is the water level due to the tidal effect, $W(t)$ is the water level due to the waves run-up, and $S(t)$ is the storm surge effect. The following sections describe the data collected and the processing methods to quantify the impact of each of the above factors, with a certain return period.

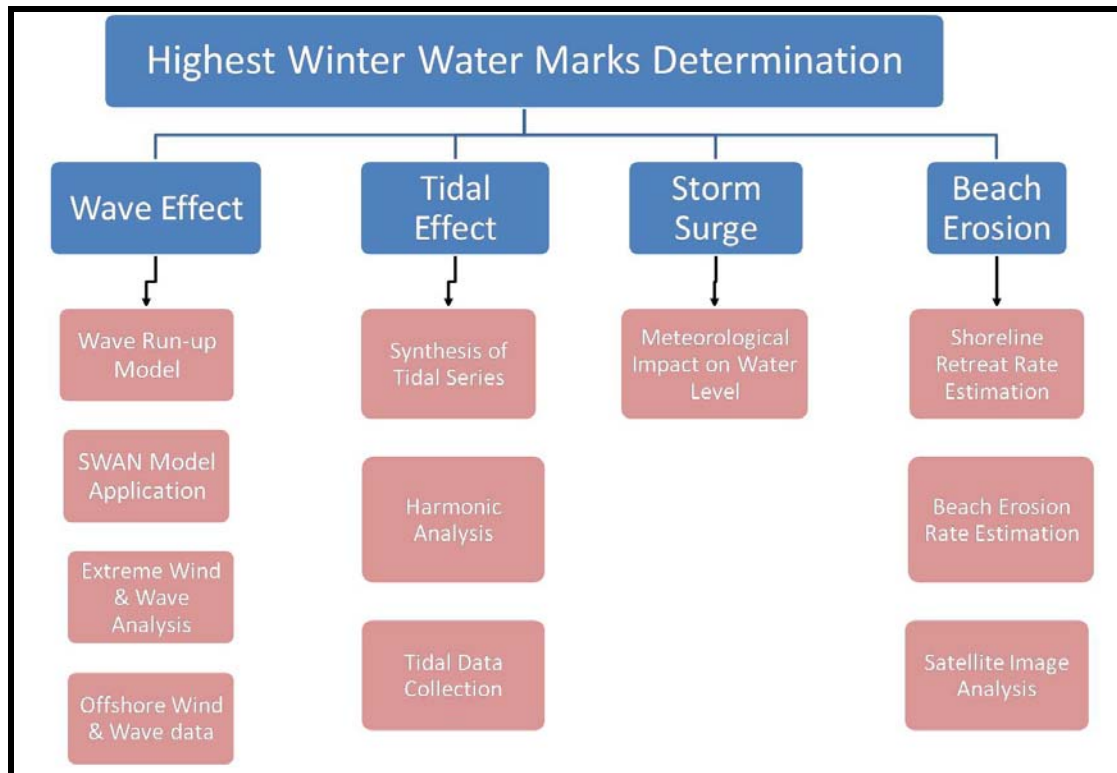


Figure 2. Methodological framework for the determination of HWWMs.

Present report proposes an analytical methodology for the HWWMs determination over rocky impermeable shores (shorelines of type C according to the geomorphologic classification). This methodology will be presented in the following sections. In the case of a sandy beach (shorelines of type A and B of the geomorphologic classification), the erosion and the retreat rates of the shoreline should be estimated. Satellite image analysis may be used to estimate the rate of erosion in the examined shoreline, and numerical models (e.g., LITPACK, Genesis, etc.) may be used to hindcast the rate of coastal retreat over the future years.

Step 4: Assessment of Ecological and Landscape Values of the Shoreline

Ecological functions of the coastal zone and coastal landscapes should be considered in the defining the setbacks along a shoreline. For example, in ecologically sensitive areas, building shall not be permitted, although some soft uses could be allowed.

Ecological importance may be valued using the NATURA 2000 network, covering most of the Marine Protected Areas and Terrestrial Reserves in the coastal zone. Coastal landscapes should also be assessed and protected, using setback lines as a tool for its delimitation (Conscience, 2010).

Step 5: Assessment of Cultural and Human Values of the Shoreline

A stricter planning and permitting policy should be applied, avoiding constructions and maintaining and protecting coastlines of ecologically-sound cultural heritage, when it is considered as a major issue by the public. Areas of significant landscape value, marine archaeological heritage sites, and coasts of cultural and scientific significance should be included in the above policy.

Step 6: Assessment of Public Uses of the Shoreline

According to the Protocol, existing buildings (urban areas, cities, historical centers, etc.) and valuable heritage and coastal uses should be not affected by new measures. Special cases should be considered and assessed. The Corine 2000 database could be used to examine the current land uses of coastal zone areas.

Step 7: Analysis of Transit and Accessibility Issues of the Shoreline

Private ownerships, which may (in some countries), restrict public use of or access to coastal resources should be considered and assessed at this stage. Although the Protocol does not specify the cases of non-application of the coastal setback zone in the already built-up areas, the successful implementation of the Article 8 requires a considerable level of flexibility.

Step 8: Analysis of Legal and Administrative Provisions

The administrative processes for the identification and implementation of setback lines should start with the identification of an institution in charge in each member state. The institution in charge is normally a regional or national organization.

Step 9: Public Involvement and Discussion

Public participation is an important tool for the integrated planning and management approaches of coastal setbacks. By involving members of the public with special interest in the determination of setback lines along a shoreline, setback planning outcomes are better accepted and policies are more likely to be complied. Public participation modes may include hearings, surveys, workshops and advisory committees, allowing the total citizen control on the final decision making.

4. Methodological Framework for HWWMs Determination

The common methods and tools for the identification of setback lines cover physical criteria for the identification of highest winter water level under certain return period scenarios, including also climate change trends. The highest winter water mark is not completely deterministic, but is based on statistic calculations about the probability of the occurrence of an extreme event. Extreme storm events with a return period of 50 years seem reasonable for the HWWMs determination. The proposed methodology for rocky, non-eroding, impermeable shorelines utilizes the Generalized Extreme Value distribution theory, wave numerical models and wave run-up estimations, as described in the steps below:

Step 1. Determination of the Offshore Extreme Wind and Wave Effect

The wave effect may be assessed by applying Extreme Value Analysis (EVA) on an offshore wind and wave time-series. In this analysis, only the independent non-overlapping storms with at least 6 h duration, exceeding a certain threshold (u) and separated by a minimum distance of 48 h between consecutive data points, may be selected. Threshold selection involves the careful inspection of the Q-Q graphs, Hill-plots and the sample-mean-excess against threshold plots. Further, following the Generalized Extreme Value distribution (GEV), assuming that the wind and wave values were independent and identically distributed (iid):

$$F(x; \mu, \sigma, \xi) = \begin{cases} \exp \left[- \left(1 + \xi \frac{x - \mu}{\sigma} \right)^{-1/\xi} \right], & \xi \neq 0, \\ \exp \left[- \exp \left(- \frac{x - \mu}{\sigma} \right) \right], & \xi = 0 \end{cases} \quad (2)$$

where $1 + \xi(x - \mu) / \sigma > 0$, μ is a location parameter, σ is a scale parameter and ξ is the shape parameter of the distribution, being independent of the selected threshold levels. The p -year return level z_p is obtained as:

$$\hat{z}_p = u + \frac{\sigma^*}{\xi^*} \left[(\lambda p)^{\xi^*} - 1 \right] \quad (3)$$

where u is the defined threshold, $\xi^* = \xi$, $\sigma^* = \sigma + \xi(u - \mu)$ and λ is the exceedance rates of threshold u , i.e., $\lambda = P(X > u)$, defined as:

$$\lambda = 1 - \exp \left\{ - \frac{1}{N} \left[1 + \xi \left(\frac{u - \mu}{\sigma} \right) \right]^{-1/\xi} \right\} \quad (4)$$

where N is the number of data exceeding threshold u . The Maximum Likelihood Estimator is usually followed for the estimation of GEV model parameters. Analysis

was performed using the package extremes in the R open source statistical software and by EVIM (Gençay et al., 2001) in Matlab.

Step 2. Determination of the Nearshore Wave Effect

To reproduce the wave field in the nearshore zone, under extreme offshore wind and wave conditions, a wave numerical model (e.g., SWAN, WAM) could be applied. SWAN is a third-generation phase-averaged spectral model SWAN was applied (Booij et al., 1999). The model solves the wave action balancing equations to generate waves and simulates the wave evolution by considering a set of physical processes, as the frequency downshift, wave shoaling and wave refraction from deep towards the nearshore waters.

$$\frac{\partial N}{\partial t} + \frac{\partial}{\partial x}(U + c_x)N + \frac{\partial}{\partial y}(V + c_y)N + \frac{\partial}{\partial \sigma}c_\sigma N + \frac{\partial}{\partial \theta}c_\theta N = \frac{S_{tot}}{\sigma} \quad (5)$$

with

$$S_{tot} = S_{in} + S_{wc} + S_{nl4} + S_{bot} + S_{brk} + S_{nl3} \quad (6)$$

where N is the wave action spectral density function; σ and θ are the angular frequency and the direction of a component wave; c_x and c_y are the group velocities in the x and y directions, respectively; c_σ and c_θ are the characteristic velocities in the σ and θ directions, respectively; S_{tot} is the source term, and U and V are the current velocities in the x and y directions, respectively; S_{in} is the transfer of energy from the wind to the waves; S_{wc} is the dissipation of wave energy due to whitecapping; S_{nl4} is the nonlinear transfer of wave energy due to quadruplet (four-wave) interaction; S_{bot} is the shallow water energy dissipation due to bottom friction; S_{brk} is the energy dissipation due to wave breaking, and S_{nl3} is the nonlinear triad (three-wave) interaction.

Step 3. Determination of Tidal and Storm Surge Effects

Hourly water level data should be collected and utilized to assess the tidal and storm surge impact on the water level in the studied area. Harmonic analysis should be performed on this dataset to determine the tidal amplitudes and phases of the various tidal harmonics. The World Tides (Boon, 2006) Matlab software was used for the harmonic analyses of these water level data. After analysis, tidal data should be re-synthesized for the same studied period, and the meteorological effect may be produced as the difference between actual measurements and the sum of the harmonic constituents.

Step 4. Determination of the Maximum Potential Wave Run-up on a Rough, Impermeable Shore

The maximum potential wave run-up on a rough, impermeable shore of medium to high slope, as the herein examined, was based on the methodology described in CEM

(Coastal Engineering Manual, U.S. Army Corps of Engineers, 2005). A new wave run-up equation was introduced by Hughes (2004) and was adopted by CEM, as:

$$\frac{R_{u2\%}}{h} = 4.4(\tan \alpha)^{0.7} \left(\frac{M_F}{\rho g h^2} \right)^{1/2} 0.505 \text{ when } 2.0 \leq \cot \alpha \leq 4.0 \quad (7)$$

where $R_{u2\%}$ is the maximum vertical run-up distance, measured from the mean sea level, exceeded by the 2% of wave run-ups; $\tan \alpha$ is the shore's slope; ρ is the water density; g is the gravitational acceleration; h is the water depth and M_F is the depth-averaged wave momentum flux (Figure 3).

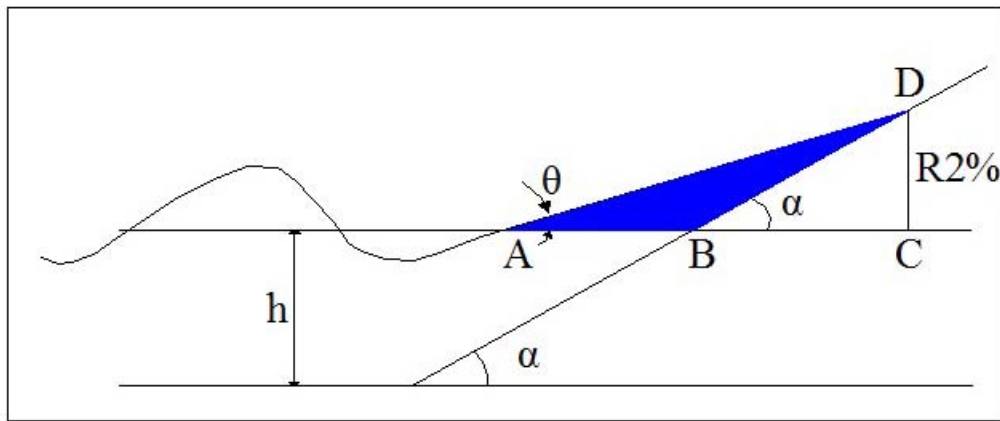


Figure 3. Maximum wave run-up on smooth impermeable plane slope (after Hughes, 2005).

The distance BC represents the wave run-up computed as the product of $R_{u2\%}$ and the sinus of shore slope α . Equation 3 is valid for shore slopes steeper than 1:4 ($\cot \alpha = 4$). For a wider range of slopes (up to 1:30) this equation was modified by Hughes (2004), as:

$$\frac{R_{u2\%}}{h} = 4.4(\tan \alpha)^{0.7} \left(\frac{M_F}{\rho g h^2} \right)^{1/2} \text{ when } 1.5 \leq \cot \alpha \leq 30 \quad (8)$$

with relatively limited accuracy than equation (3).

The parameter $\left(\frac{M_F}{\rho g h^2} \right)$ in Equations (3) and (4) represents the non-dimensional wave momentum flux for finite amplitude, non-linear waves. This parameter may be substituted as:

$$\left(\frac{M_F}{\rho g h^2} \right) = A_0 \left(\frac{h}{g T_p^2} \right)^{-A_1} \quad (9)$$

where the coefficients A_0 and A_1 are coefficients, as:

$$A_0 = 0.639 \left(\frac{H_{m0}}{h} \right)^{2.026} \quad (10)$$

and

$$A_1 = 0.180 \left(\frac{H_{m0}}{h} \right)^{-0.391} \quad (11)$$

where h is the water depth, from mean sea level, at the toe of the slope, H_{m0} is the incident significant wave height, g is the gravitational acceleration and T_p is peak wave period.

5. Case Study: The Kavala Municipality shoreline

5.1. Site Description for Case Study Implementation

Kavala Municipality is located at the northern part of Greece, near the borders with Turkey and Bulgaria (Figures 4 and 5). The broader area borders to the north with the Pagon Mountain, famous for its gold mines during the Alexander the Great era, to the east with the River Nestos and to the west with the Strymon River, two transboundary rivers originating from Bulgaria and FYROM, respectively. To the south one can view the Gulf of Kavala, the second in size semi-enclosed coastal water body of the Thracian Sea, which is part of the North Aegean Sea's continental shelf (Sylaios et al., 2012).

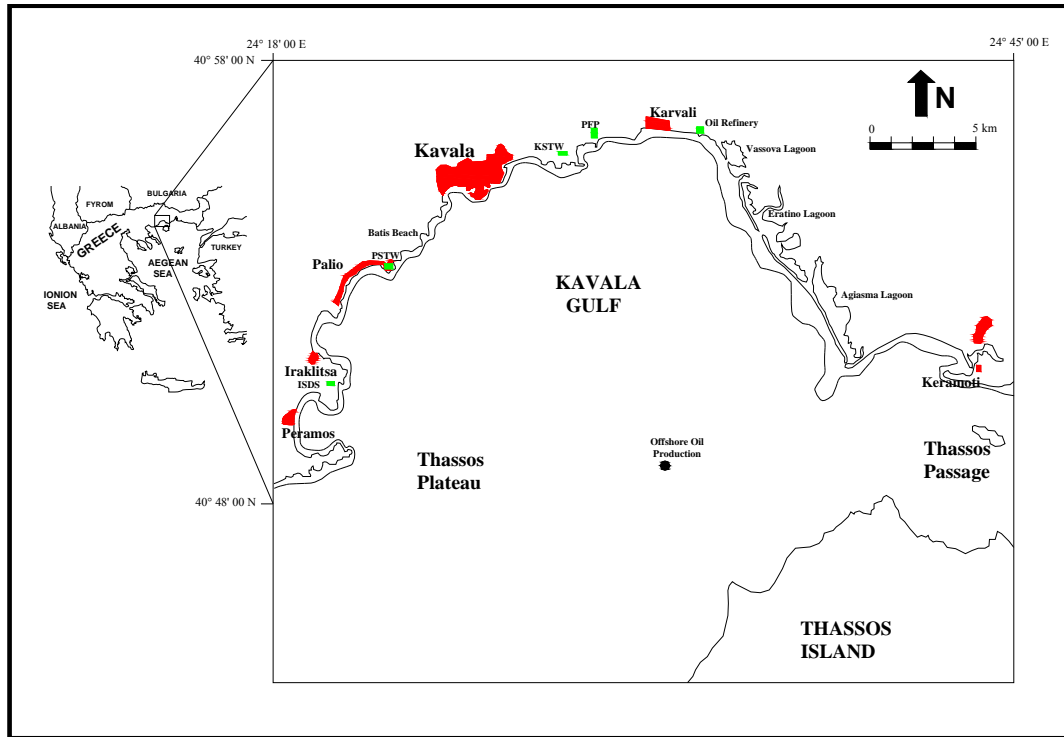


Figure 4. Coastal zone of Kavala Gulf and Kavala Municipality.

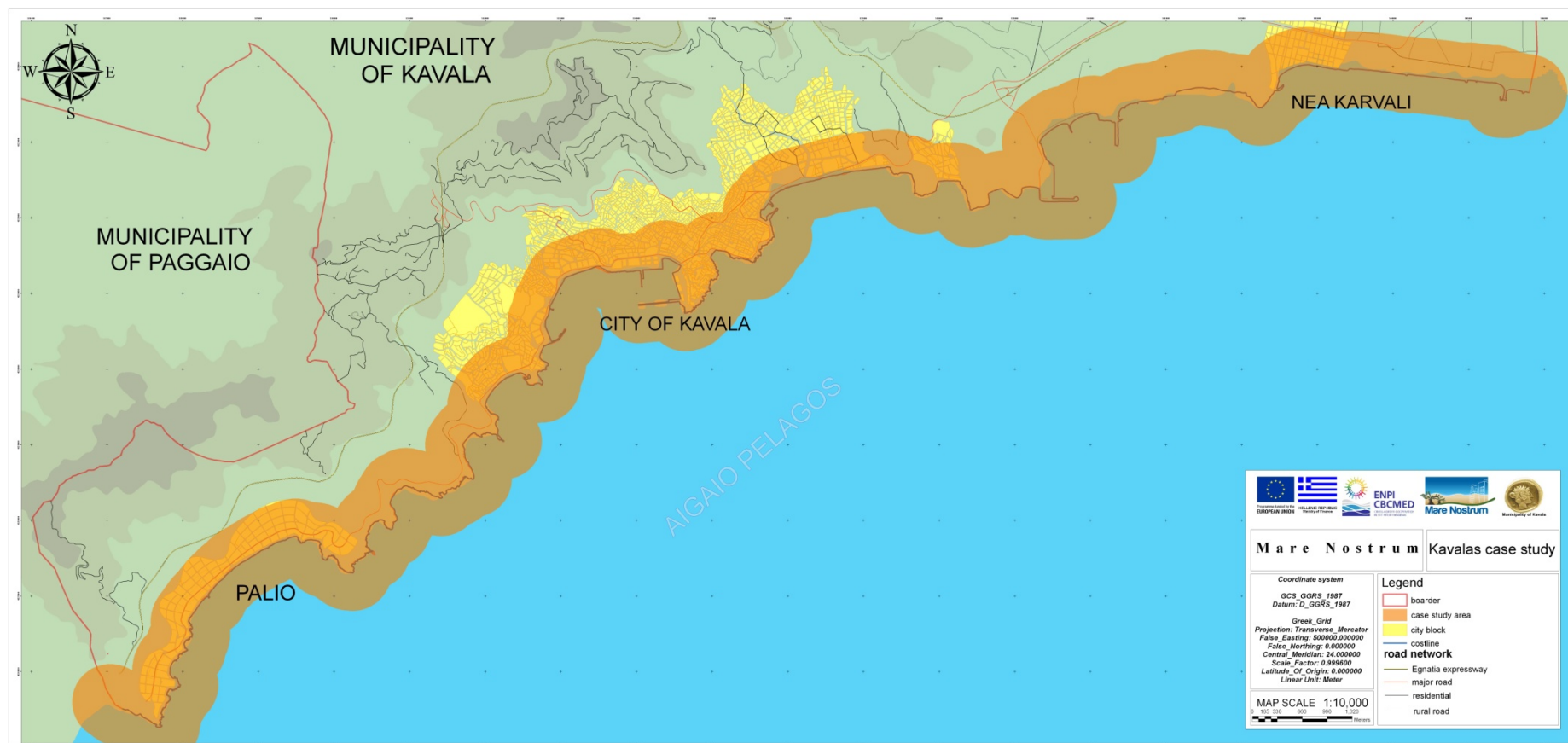


Figure 5. The coastal zone of Kavala Municipality.

The gulf and its coastal zone is rich in natural ecosystems, developing along the 65-km long coastline. The Gulf's basin has an amphitheatric shape, with gentle slopes at the center, increasing rapidly towards the coast, and a symmetry axis directed NNE-SSW (Sylaios et al., 2005).

The climate of the broader area is characterized as intermediate between Mediterranean and continental type (Mariopoulos, 1982), dominated by moderate precipitation, cold winters, and arid summer periods. Eastern and northwestern wind directions are dominant during the winter period having frequencies of 7% and 10%, respectively. The area is micro-tidal, with tidal range varying between 0.12 m during neap tides and 0.30 m during spring tides under the prevalence of the semi-diurnal (M_2) tidal constituent. The input of Black Sea Water (BSW) through the Dardanelles governs the surface dynamics of Kavala Gulf by supplying low salinity (29–34), nutrient-rich BSW, which occupies the surface layer of the water column (20–40 m) (Sylaios, 2011).

The examined coastline lies at the central-eastern zone of Kavala Municipality, between the old municipal hospital and a small marina. It is a mildly steep, rocky (granite), impermeable shore, directly exposed to the waves of the open North Aegean Sea, where houses are built from 1920s. The shore was selected as a case study, since several legal disputes have taken place during the latest decades, among property owners and the state, on the exact definition of the baseline and the setback line (Figure 6).

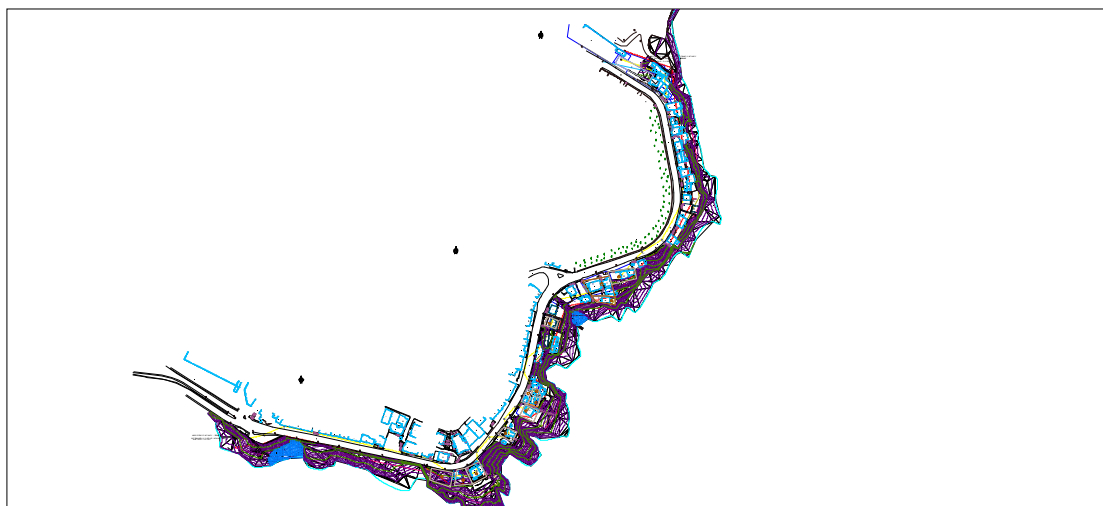


Figure 6. The examined coastline of Kavala Municipality.

5.2. Tidal and Storm Surge Effect

Harmonic analysis was performed on the hourly tidal data recorded in Kavala harbor, and the wind and storm surge effects on the water level variability were produced. Figure 7 illustrates a sample of the recorded and reconstructed - through harmonic

analysis - time-series, together with the non-tidal effect, presented by the low-pass-filtered residual time-series. Frequency analysis on the non-tidal time-series depicted that a maximum increase in sea level of 0.75 m (related to mean sea level), due to storm surge events, may occur in the studied area. In case such event occurs during the high water period of spring tides, an additional increase in sea level of 0.20 m is expected.

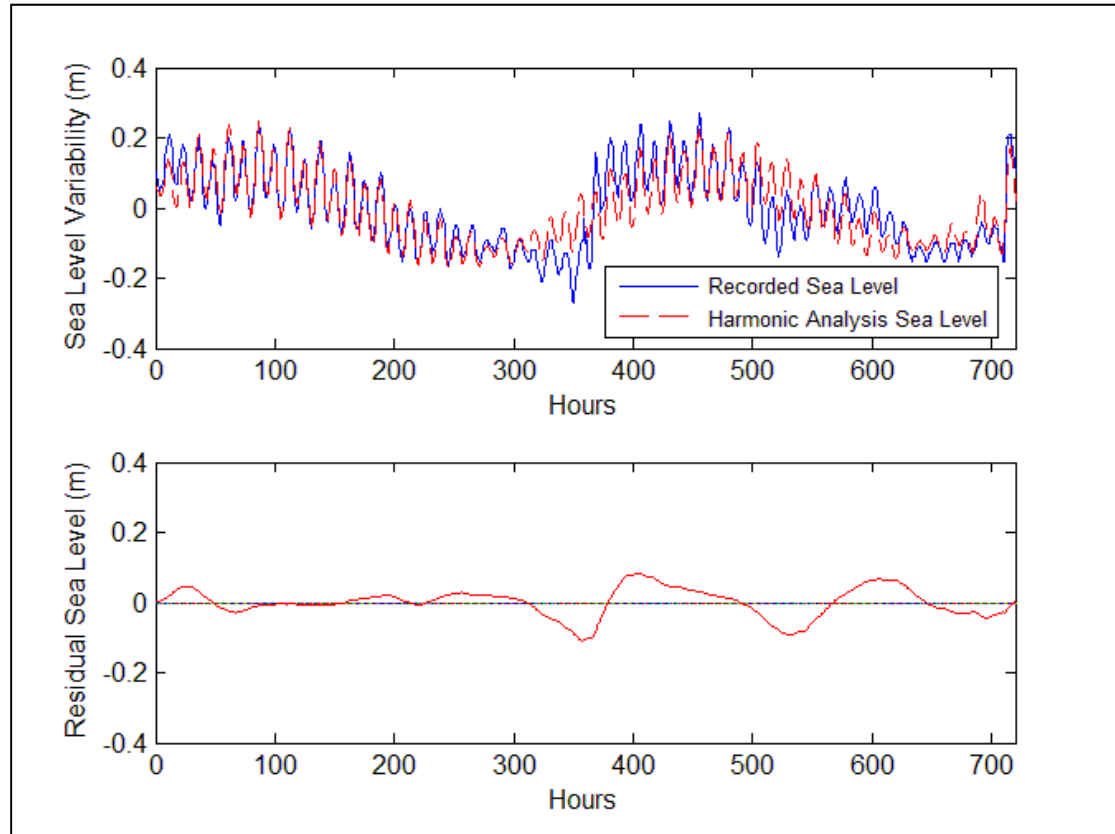


Figure 7. Monthly variability of tidal and reconstructed signals (upper panel) and residual storm surge effect (lower panel) in Kavala Harbor.

5.3. Extreme Offshore Wind and Wave Analysis

Eleven years offshore wind and wave data (2000-2010) were collected by an oceanographic platform of the POSEIDON sea observatory network, located near Athos Peninsula (39.961°N, 24.721°E, 220 m depth). The platform recorded with 3-hrs interval wave parameters (spectral significant wave height H_{m0} , the mean zero-up-crossing T_{02} , and the mean wave direction θ_w) and wind parameters (gust wind speed, wind speed and wind direction), recorded at 3 m height above sea level (Soukissian et al., 2002). Sylaios et al. (2009) utilized this dataset to simulate the wind-wave relationships and produce short-term wave forecasts, through a fuzzy logic model. Overall, 14,128 wind measurements and 10,459 wave measurements were obtained

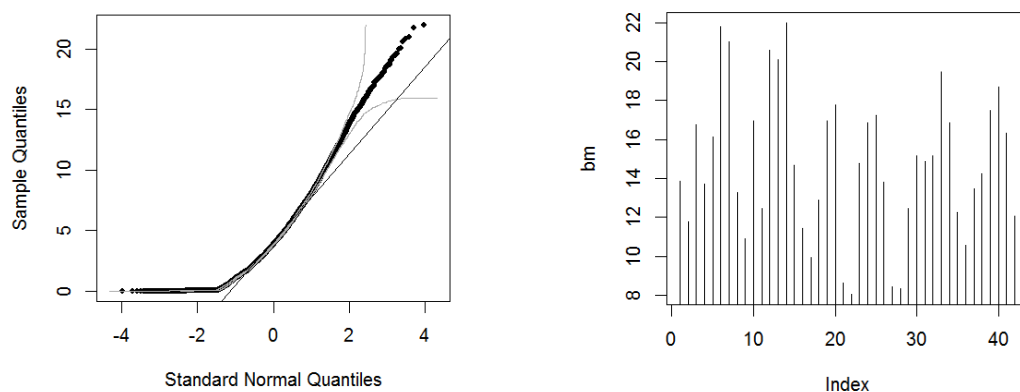
and imported in the extreme wind and waves analysis system, aiming to determine the extreme meteorological and wave events with a return period of 25, 50 and 100 years.

Statistical analysis on the wind and wave records of POSEIDON buoy produced the results summarized in Table 2. Extreme Value Analysis on the wind and wave data using the thresholds of 12 m/s for the wind series and 3.2 m for the significant wave height produced the GEV parameters summarized in Table 3. The fact that $\xi < 0$ suggests that the wind speed tail is approximated by the Weibull distribution. On the other hand, a heavy-tailed distribution in the extreme wave values is obtained, as the shape parameter $\xi > 0$. Using these GEV parameters and Equation (3), the extreme offshore wind and wave events for a certain return period were approximated.

Table 2. Statistical parameters of wind and wave datasets recorded from POSEIDON buoy (North Aegean Sea) during 2000-2010.

Parameter	Wind Speed (m/s)	Significant Wave Height (m)
Minimum Value	0.000011	0.03616
1 st Quantile	1.696000	0.28920
Median	3.829000	0.57130
Mean	4.530000	0.82920
3 rd Quantile	6.573000	1.10900
Maximum	21.960000	5.50500

Figure 8 presents the statistical analysis on the offshore meteorological dataset.



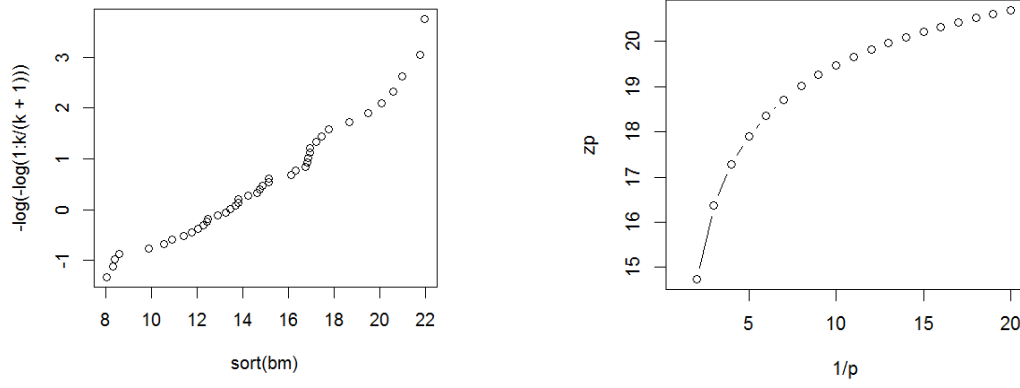


Figure 8. Statistical analysis on the offshore meteorological data.

Table 3. Parameters of the Generalized Extreme Value distribution for the offshore wind and wave datasets.

Parameters	Wind Speed (m/s)	Significant Wave Height (m)
μ , location parameter	13.4873856 ± 0.6343573	1.8687433 ± 0.08695899
σ , scale parameter	3.6335170 ± 0.4635625	0.7503513 ± 0.06992173
ξ , shape parameter	-0.2945518 ± 0.1260640	0.2038059 ± 0.09424234

As seen in Figure 9 where the diagnostic plots obtained from the application of the GEV model on the offshore wind dataset are presented, three values were produced for each return period (minimum, maximum and mean). Results for return periods of 25, 50 and 100 years are shown in Table 4. For the determination of the highest winter water marks on an impermeable shoreline, the mean value of the extreme wind and wave events with return period of 50 years was selected. These values were imported as boundary conditions on the outer, low resolution computational grid of the SWAN numerical model.

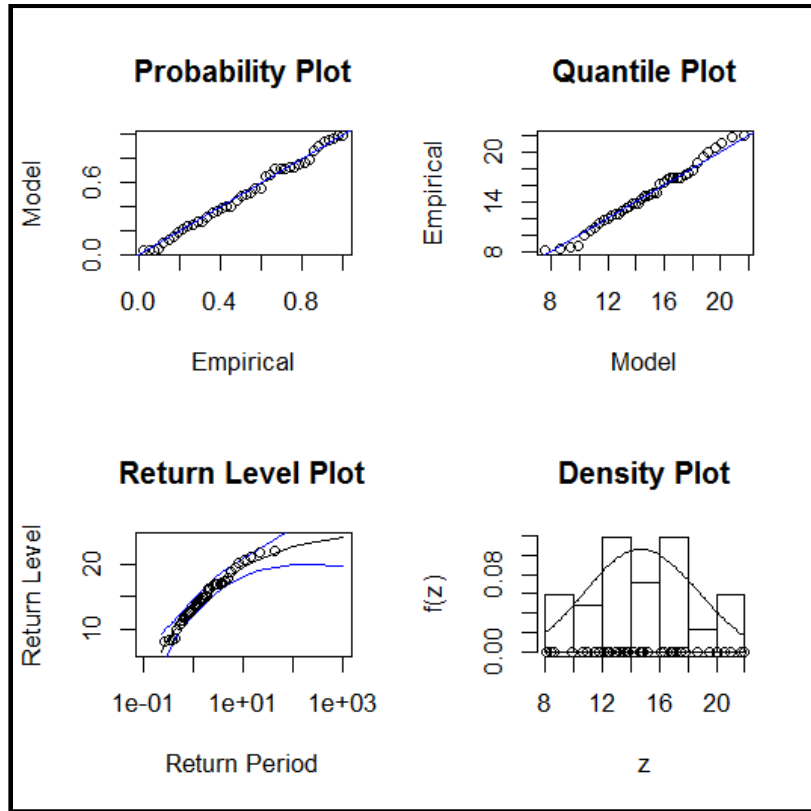


Figure 9. Diagnostic plots obtained from the application of the GEV model on the offshore wind dataset.

Table 4. Extreme values of wind speed (in m/s) and significant wave height (in m) for various return periods (offshore North Aegean Sea).

Return (yrs)	Period	Wind Speed (m/s)			Significant Wave Height (m)		
		Min	Mean	Max	Min	Mean	Max
25		19.096	22.059	26.067	5.282	6.510	8.191
50		19.467	22.765	27.435	6.068	7.779	10.227
100		19.743	23.334	28.641	6.911	9.228	12.702

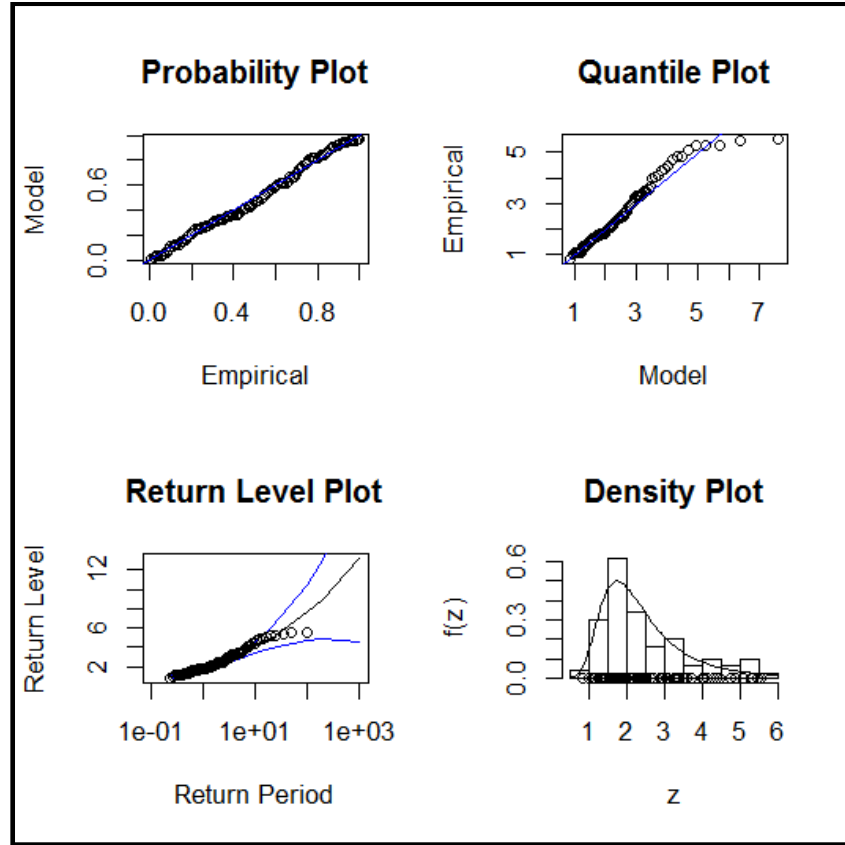


Figure 10. Diagnostic plots obtained from the application of the GEV model on the offshore wave dataset.

5.4. Nearshore Extreme Wave Characteristics at the Study Area

The SWAN wave model was implemented with the nominal formulations of the physical processes, to describe the wave characteristics at the nearshore zone of Kavala coastline. In order to achieve the required spatial downscaling for the produced wave field, three rectangular bilinear grids of increasingly higher resolution were used. The coarse grid covers the entire study area (North Aegean Sea), the second medium nested grid covers the Western Thracian Sea, including Thassos Island, and the third fine resolution grid focuses on the studied coastline of Kavala Municipality (Figure 11). The geometric and geographical characteristics for each grid of the above described triple nesting are shown in Table 5.

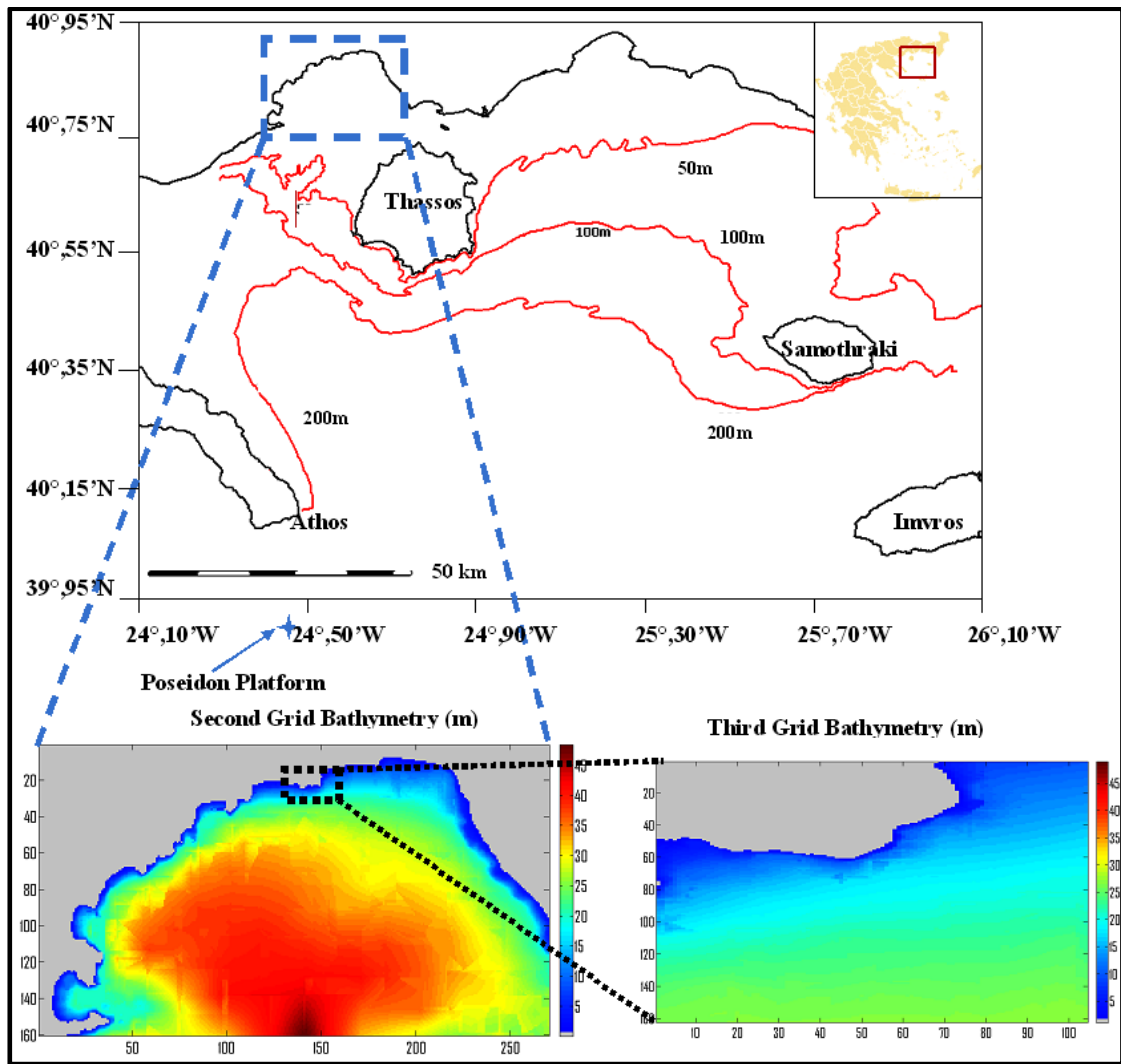


Figure 11. Computational grids of the nested SWAN model.

Table 5. Computational grids for SWAN model implementation in Kavala Municipality coastline.

Grid Description	Dimensions (Easting × Northing)	Cell Grid Size (dx = dy)	Geographic Co-ordinates	Boundary Conditions Imposed
Coarse Resolution Grid	164 km × 112 km	1,000 m	40° 95' N, 24° 10' E – SW point 39° 95' N, 26° 10' E – NE point	Extreme values for significant wave height, period and direction; extreme wind values at all grid points.
Medium Resolution Grid	27 km × 16 km	100 m	40° 57' 55'' N, 24° 17' 47'' E – SW point 40° 85' 57'' N, 24° 35' 38'' E – NE point	Model output from the coarse resolution grid along all open boundaries; extreme wind data at all grid points.
Fine Resolution Grid	0.45 km × 1.17 km	10 m	40° 56' 24'' N, 24° 25' 05'' E – SW point 40° 55' 2'' N, 24° 25' 12'' E – NE point	Model output from the medium resolution grid along all open boundaries; extreme wind data at all grid points.

The spatial distribution of significant wave heights and wave propagation direction over the Thracian Sea (coarse grid), for extreme waves (mean value with 25 years return period) propagating from the southern direction, is shown in Figure 12. Thassos and Samothraki Islands induce significant sheltering effects in the broader area reducing the wave heights by almost 40%. The eastern part of Kavala Gulf appears affected by this sheltering effect. Figures 13 and 14 illustrate the spatial wave field under extreme events with return period of 50 and 100 years, respectively.

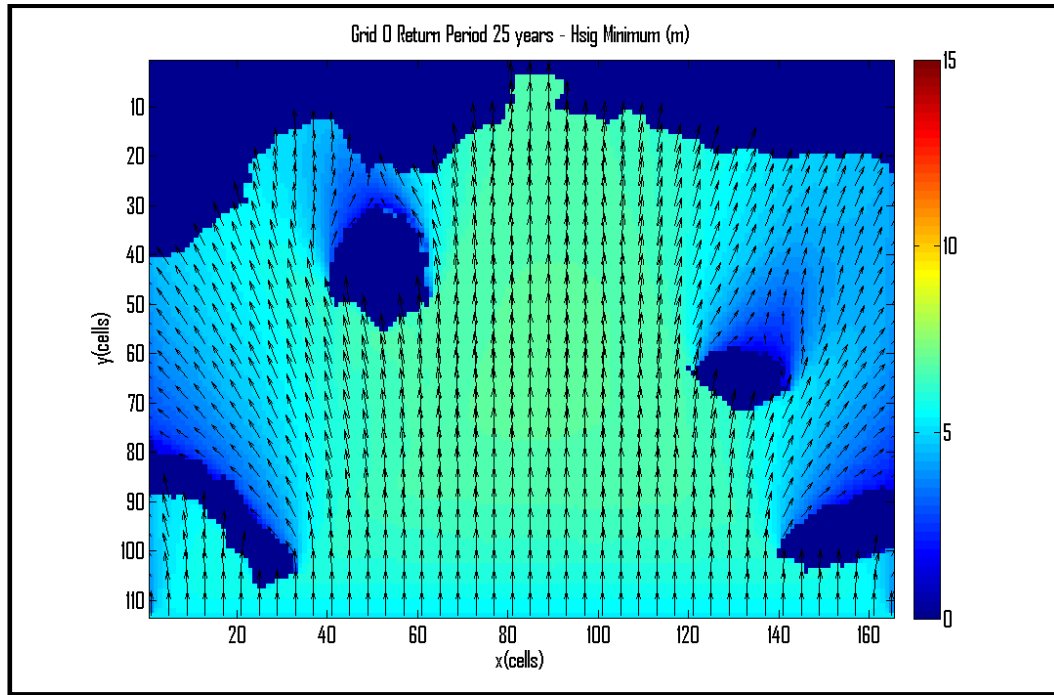


Figure 12. Spatial distribution of significant wave height and direction in the North Aegean Sea for northward propagating waves, during an extreme wind and wave event, with return period 25 years (minimum value).

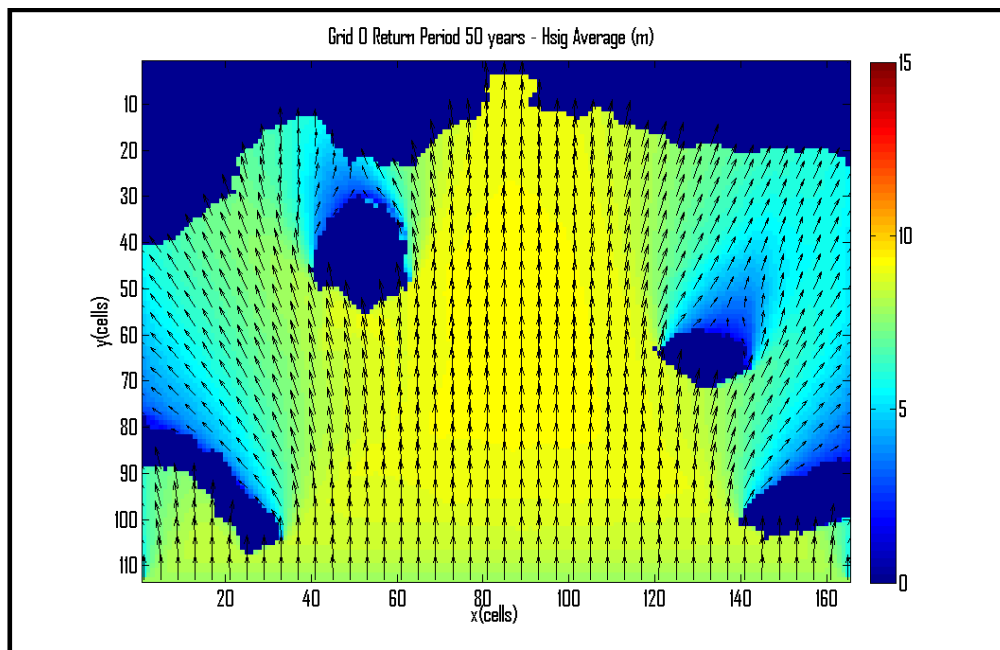


Figure 13. Spatial distribution of significant wave height and direction in the North Aegean Sea for northward propagating waves, during an extreme wind and wave event, with return period 50 years (mean value).

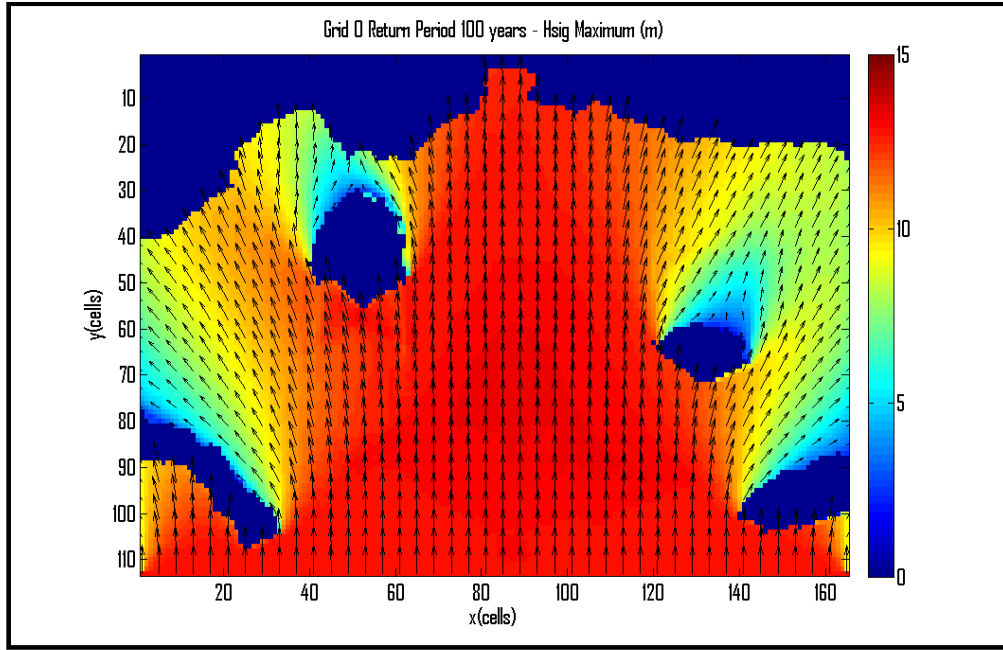


Figure 14. Spatial distribution of significant wave height and direction in the North Aegean Sea for northward propagating waves, during an extreme wind and wave event, with return period 100 years (maximum value).

The distribution of the wave field in Kavala Gulf under the 25-years return period extreme event is revealed from the medium-scale computational grid (Figure 15). The western part of the gulf exhibits higher wave heights ($H_s \sim 6.2$ m), with slightly deviated propagation to the north-west, due to wave refraction. At the central part of the gulf southern waves with $H_s \sim 5.5$ m are incident to the shoreline of interest, while further eastwards wave heights diminish up to 3.2 m with propagation directions deflected to the north-east. Figures 16 and 17 illustrate the spatial wave field under extreme events with return period of 50 and 100 years, respectively.

Finally, the distribution of the wave field at the smaller, fine resolution grid covering the nearshore zone of the examined case study, under the 25-years return period extreme event, is shown in Figure 18. Incident waves reach the shoreline of the study area propagating to the north-west with $H_s \sim 7.0 - 7.2$ m. The incident wave height at each 10 m nearshore cell, combined to the tidal and storm surge effects, was used as boundary condition for the wave run-up model. Figures 19 and 20 show the significant wave height and direction of propagation distribution at the nearshore zone during extreme events of 50 and 100 years return period, respectively.

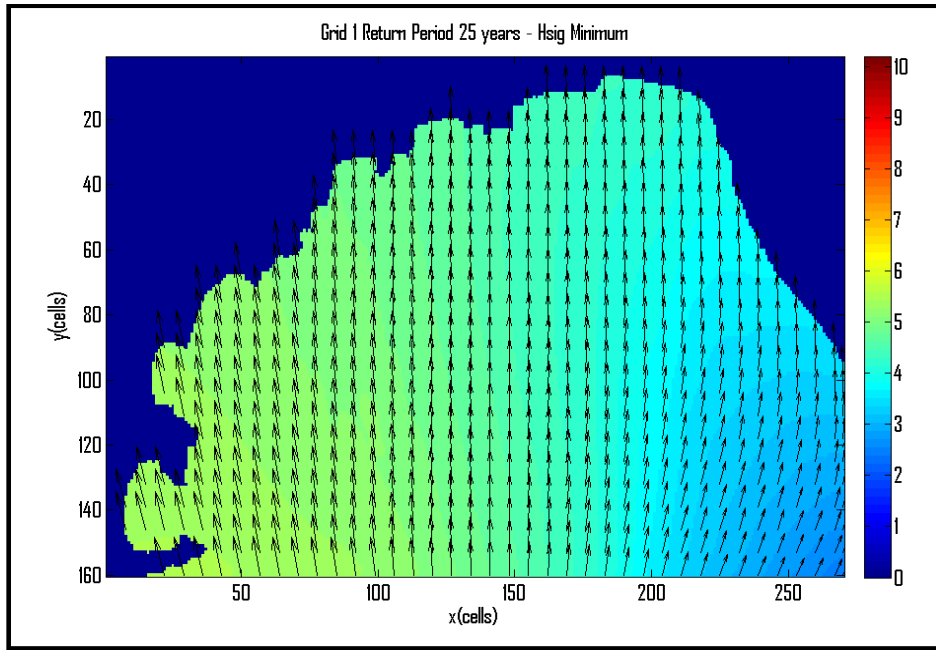


Figure 15. Spatial distribution of significant wave height and direction in Kavala Gulf for northward propagating waves, during an extreme wind and wave event, with return period 25 years (minimum value).

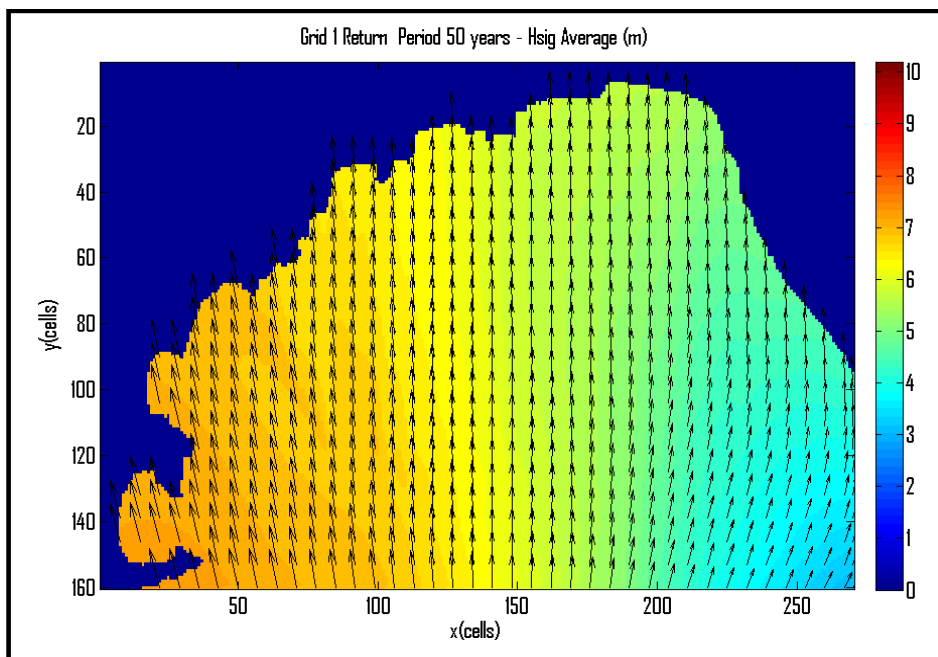


Figure 16. Spatial distribution of significant wave height and direction in Kavala Gulf for northward propagating waves, during an extreme wind and wave event, with return period 50 years (mean value).

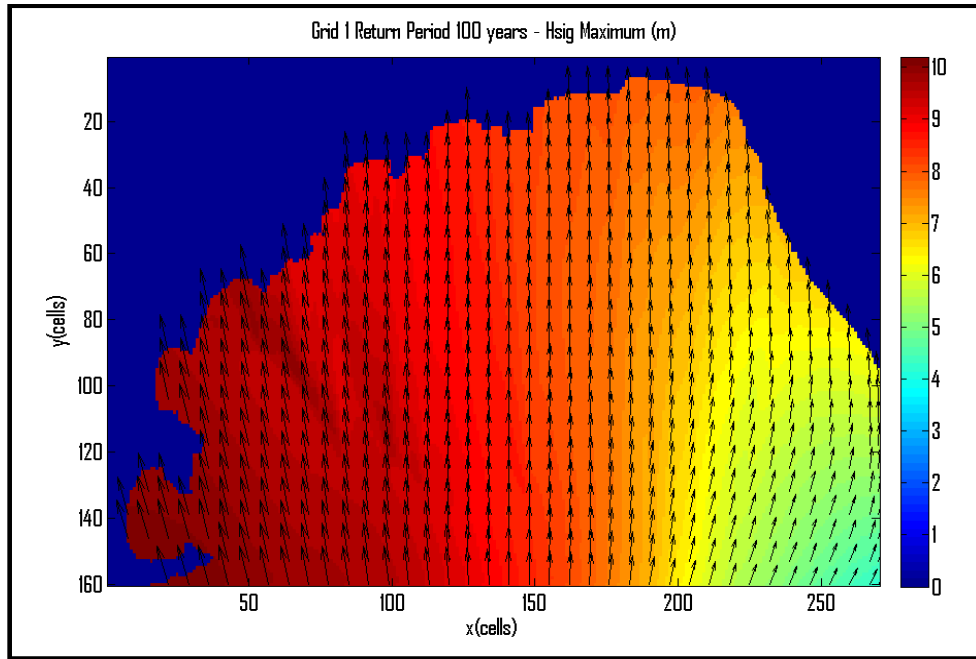


Figure 17. Spatial distribution of significant wave height and direction in Kavala Gulf for northward propagating waves, during an extreme wind and wave event, with return period 100 years (maximum value).

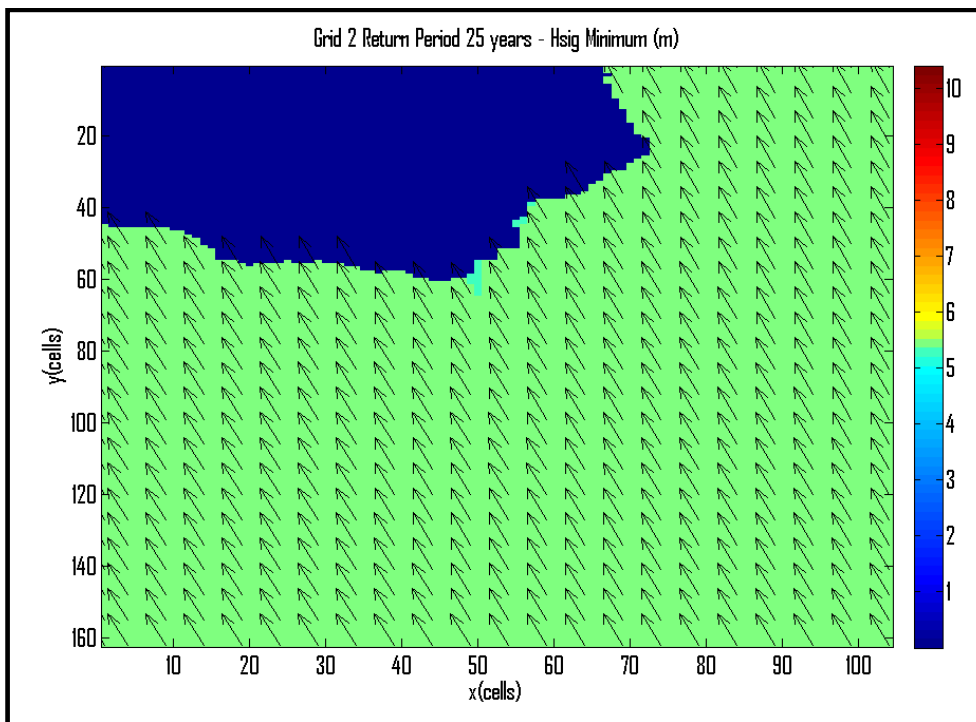


Figure 18. Spatial distribution of significant wave height and direction at the nearshore zone of Kavala Municipality for northward propagating waves, during an extreme wind and wave event, with return period 25 years (minimum value).

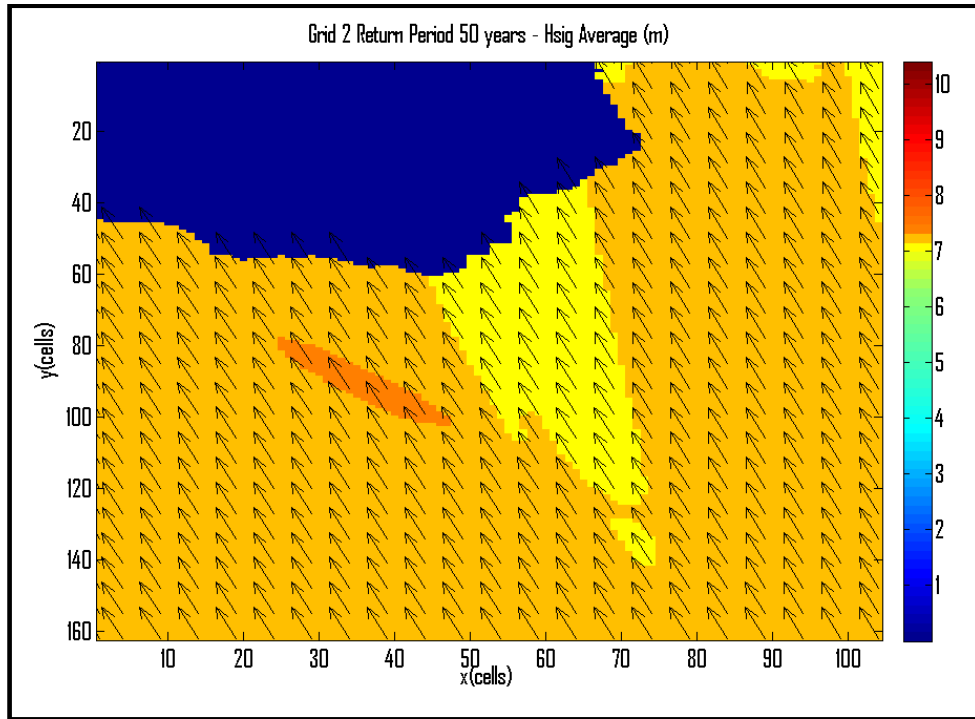


Figure 19. Spatial distribution of significant wave height and direction at the nearshore zone of Kavala Municipality for northward propagating waves, during an extreme wind and wave event, with return period 50 years (mean value).

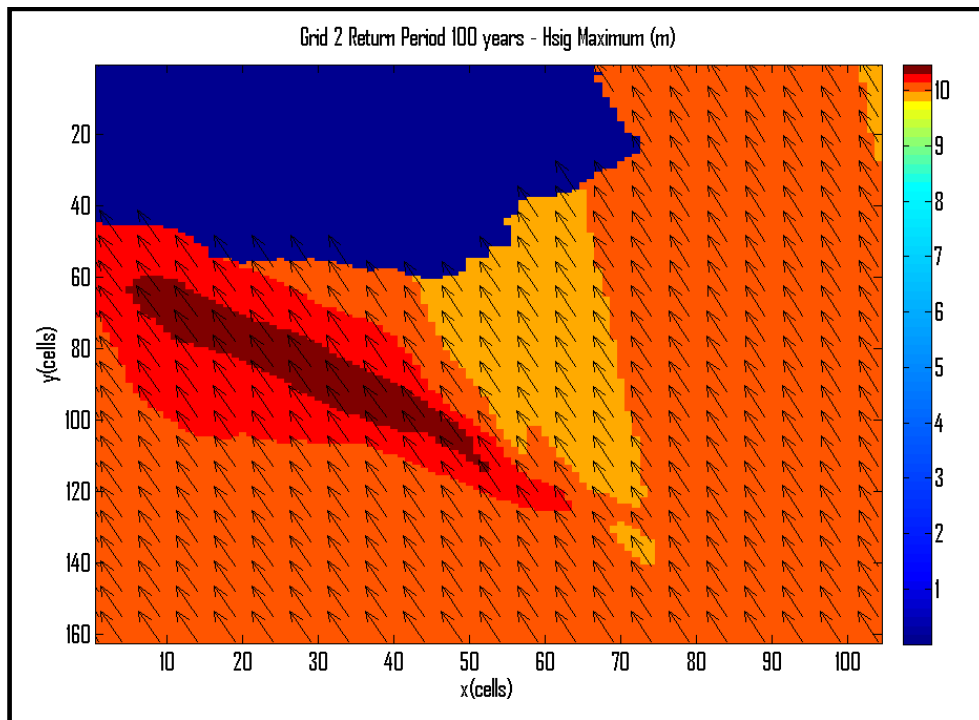


Figure 20. Spatial distribution of significant wave height and direction at the nearshore zone of Kavala Municipality for northward propagating waves, during an extreme wind and wave event, with return period 100 years (maximum value).

5.5. Determination of Maximum Wave Run-up in the Case Study Area

Three baselines for setback determination were considered in this analysis: a) the maximum wave run-up during an extreme event with a return period of 25 years (minimum value); b) the maximum wave run-up during an extreme event with a return period of 50 years (mean value); and c) the maximum wave run-up during an extreme event with a return period of 100 years (maximum value). These lines were drawn by applying the wave run-up model considering the combined tidal, storm surge and wave effect in the study area. Figure 21 represents the configuration of these lines along the whole shoreline.

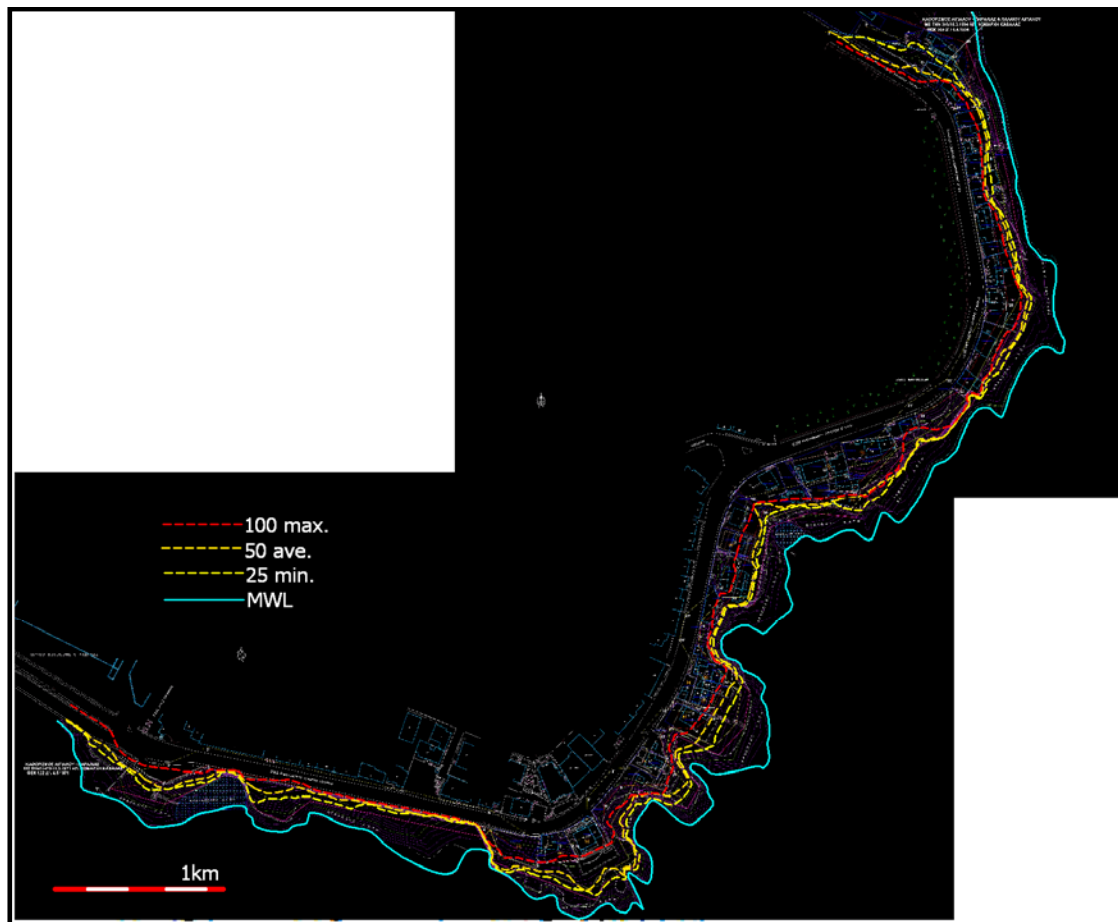


Figure 21. The Kavala Municipality shoreline with a) the mean sea level (blue line), and the lines of maximum wave run-up, as a) under the 25-years return period (yellow line), b) the 50-years return period (orange line), and c) the 100-years return period (red line).

Indicative parts of the examined shoreline are shown in Figures 22 and 23. All three derived lines were imported and geo-referenced on the initial topographic GIS mapping.



Figure 22. Eastern part of the Kavala Municipality shoreline with a) the mean sea level (blue line), and the lines of maximum wave run-up, as a) under the 25-years return period (yellow line), b) the 50-years return period (orange line), and c) the 100-years return period (red line).

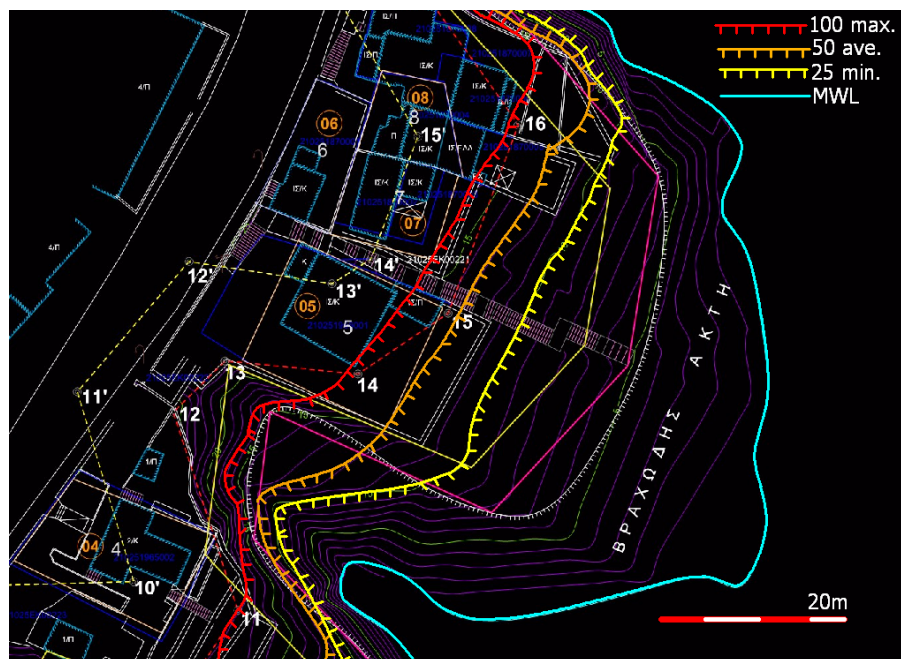


Figure 23. Western part of the Kavala Municipality shoreline with a) the mean sea level (blue line), and the lines of maximum wave run-up, as a) under the 25-years return period (yellow line), b) the 50-years return period (orange line), and c) the 100-years return period (red line).

References

- Alpan, H., 2011. Comparing the utility of image algebra operations for characterizing landscape changes: The case of the Mediterranean coast. *Journal of Environmental Management* 92, 2961-2971.
- Booij, N., Ris, R.C., Holthuijsen, L.H., 1999. A third-generation wave model for coastal regions. 1. Model description and validation. *Journal of Geophysical Research* C104, 7649–7666.
- Boon, J.D., 2006. *World Tides User Manual v1.01*, USA, 24 p.
- Bridge, L., Salman, A., 2010. *Policy Instruments for ICZM in Nine Selected European Countries*. Leiden, The Netherlands, Dutch National Institute for Coastal & Marine Management (RIKZ).
- Cambers, G., 1997. *Planning for Coastline Change: Guidelines for Construction Setbacks*. Environment and Development in Coastal Regions and Small Islands (CSI).
- Coastal Engineering Manual, 2005. *Estimating Irregular Wave Runup on Rough, Impermeable Slopes*, U.S. Army Corps of Engineers, ERDC/CHL CHETN-III-70, 12 p.
- Conscience, 2010. *On the use of setback lines for coastal protection in Europe and the Mediterranean: practice, problems and perspectives*. Deltares, The Netherlands, 30 p.
- FAO, 2006. *Integrated coastal management law. Establishing and strengthening national legal frameworks for integrated coastal management*. FAO Legislative Study No. 93, Rome, 274 p.
- Gençay, R., Selçuk, F., Ulugülyağci, A., 2001. EVIM: A Software Package for Extreme Value Analysis in MATLAB. *Studies in Nonlinear Dynamics and Econometrics* 5, 213-239.
- Hughes, S.A., 2004. Estimation of wave run-up on smooth, impermeable slopes using the wave momentum flux parameter. *Coastal Engineering* 51(11), 1085-1104.
- Mariopoulos, I., 1982. *The Climate of Greece*. Greek National Printing Office, Athens.
- Plan Bleu, 2005. *A Sustainable Future for the Mediterranean. The Blue Plan's Environment and Development Outlook*, edited by G. Benoit & A. Comeau. London: Earthscan. Chapter on "Coastal Areas", pp. 303-356. www.planbleu.org.
- Rabenold, C., 2013. Coastal Zone Management: Using no-built areas to protect the shorefront. *Coastal Management* 41(3), 294-311.
- Rochette, J., Billé, R., 2010. Analysis of the Mediterranean ICZM Protocol: At the crossroads between the rationality of provisions and the logic of negotiations. Institute

for Sustainable Development and International Relations (IDDRI), IDDRI SciencePo., 26 p.

Sanò, M., Marchand, M., Medina, R., 2010. Coastal setbacks for the Mediterranean: a challenge for ICZM. *Journal of Coastal Conservation* 14, 33-39.

Sanò, M., Jiménez, J.A., Medina, R., Stanica, A., Sanchez-Arcilla, A., Trumbic, I., 2011. The role of coastal setbacks in the context of coastal erosion and climate change. *Ocean and Coastal Management* 54, 943-950.

Soukissian, T.H., Prospathopoulos, A.M., Diamanti, C., 2002. Wind and wave data analysis for the Aegean Sea—preliminary results. *The Global Atmosphere and Ocean System* 8, 163–189.

Sylaios G., Stamatis, N., Kallianiotis, A., Vidoris, P., 2005. Monitoring and assessment of land-based nutrient loadings, distributions and cycling within Kavala Gulf. *Water Resources Management* 19(6), 713-735.

Sylaios, G., Bouchette, F., Tsihrintzis, V.A., Denamiel, C., 2009. A fuzzy inference system for wind-wave modeling. *Ocean Engineering* 36, 1358-1365.

Sylaios, G., 2011. Meteorological influence on the surface hydrographic patterns of the North Aegean Sea. *Oceanologia* 53(1), 57-80.

Sylaios, G., Kamidis, N., Stamatis, N., 2012. Assessment of trace metals contamination in the suspended matter and the sediments of a semi-enclosed Mediterranean Gulf. *Soil & Sediment Contamination: An International Journal* 21, 673-700.

UNEP – United Nations Environmental Program, 2008. Protocol on Integrated Coastal Zone Management in the Mediterranean.

UNEP - United Nations Environmental Program, 2012. State of the Mediterranean Marine and Coastal Environment. Mediterranean Action Plan - Barcelona Convention, Athens, 2012, 96 p.